PHYSICAL REVIEW E **90**, 040302(R) (2014)

Phase separation of fluids in porous media: A molecular dynamics study

Shaista Ahmad,[1] Sanjay Puri,[1] and Subir K. Das[2]
[1]*School of Physical Sciences, Jawaharlal Nehru University, New Delhi 110067, India*
[2]*Theoretical Sciences Unit, Jawaharlal Nehru Centre for Advanced Scientific Research, Jakkur P.O., Bangalore 560064, India*
(Received 21 August 2014; published 22 October 2014)

We present comprehensive molecular dynamics results for phase-separation kinetics of fluids in a porous medium. This system is modeled by a symmetric Lennard-Jones fluid mixture with a quenched random field. The presence of disorder slows down domain growth from power-law to a logarithmic form. It also modifies the correlation functions and structure factors which characterize the morphology. In particular, the structure-factor tail shows a non-Porod behavior, which is the consequence of scattering from rough interfaces.

DOI: 10.1103/PhysRevE.90.040302 PACS number(s): 64.75.Gh, 47.56.+r, 64.60.De

When one quenches a homogeneous binary $(A + B)$ mixture inside the miscibility gap, the system becomes thermodynamically unstable and undergoes phase separation. Its evolution towards the segregated state is characterized by the emergence and growth of domains of like particles [1–4]. The domain growth law [behavior of the characteristic length scale $\ell(t)$ with time t] depends upon various system properties, e.g., conservation laws, hydrodynamic effects, presence of disorder, etc.

The growth laws for pure and isotropic systems are well understood: $\ell(t)$ increases in a power-law fashion, viz., $\ell(t) \sim t^{\alpha}$ [1–4]. In the case of conserved order parameter with diffusive kinetics, $\alpha = 1/3$, which is referred to as the Lifshitz-Slyozov (LS) growth law [5]. The LS law applies for phase-separating solid mixtures. For fluids and polymers, the growth is much faster at later times due to the influence of hydrodynamics, and there are two additional regimes with $\alpha = 1$ [6] and $2/3$ [7]. These are referred to as the *viscous hydrodynamic* and *inertial hydrodynamic* regimes, respectively. In recent works [8], we have convincingly demonstrated via molecular dynamics (MD) simulations that there is a crossover from the diffusive to the viscous hydrodynamic regime for fluid-fluid phase separation.

Of course, real experimental systems are never pure and contain different kinds of immobile or mobile impurities. In this context, there have been a number of studies investigating diffusion-driven coarsening in Ising systems with quenched disorder, e.g., bond, site, random-field [9–21]. A general observation in these studies is that trapping of domain boundaries by disorder sites [9,10] results in a slower growth of domains. It is now well established that the growth law in disordered Ising systems crosses over from a power-law behavior to a logarithmic one [20,21].

To the best of our knowledge, there are no studies of phase-separation kinetics in fluids with quenched disorder. This system offers interesting possibilities because of its experimental importance. Further, there are important theoretical issues concerning the crossover from pure fluidic systems with their multiplicity of growth exponents to the disordered case. In this Rapid Communication, we undertake a MD study of segregation kinetics in fluids with disorder. Our MD simulations have the advantage of naturally incorporating hydrodynamic effects. We use a random-field disorder, which puts our equilibrium system in the universality class of the *random-field Ising model* (RFIM), which is analogous to *fluid mixtures in porous media* [22–26]. The latter system is of great scientific and technological interest, especially in the oil-extraction industry. Apart from porous media, the RFIM has many applications in the context of structural transitions, metal-insulator transitions, etc.

For our MD simulations, we employ a symmetric $A + B$ mixture with a high particle density: $n = N/V = 1$, N and V being the number of particles and volume of the system, with particle diameter $\sigma = 1$. Particles of equal mass (m), located at $\vec{r}_i$ and $\vec{r}_j$, interact via the potential

$$V(r) = U(r) - U(r_c) - (r - r_c)\left.\frac{dU(r)}{dr}\right|_{r=r_c}, \quad r < r_c,$$
$$= 0, \qquad r > r_c, \tag{1}$$

where

$$U(r) = 4\varepsilon_{\alpha\beta}\left[\left(\frac{\sigma}{r}\right)^{12} - \left(\frac{\sigma}{r}\right)^{6}\right] \tag{2}$$

is the Lennard-Jones (LJ) potential. Here, $r = |\vec{r}_i - \vec{r}_j|$ and $r_c = 2.5\sigma$; $\alpha, \beta = A, B$ and $\varepsilon_{AA} = \varepsilon_{BB} = 2\varepsilon_{AB} = \varepsilon$. (We set m, ε and k_B to unity in further discussions.) This particular choice of the interaction strengths energetically favors phase separation, which sets in at the critical temperature $T_c \simeq 1.42$ [27–29]. Due to the high density, this is far away from the gas-liquid transition. We have also checked that the solid-liquid transition does not occur in the temperature range of interest to us. We work with a 50:50 mixture of A and B particles $(N_A = N_B = N/2)$, corresponding to the critical composition of the system.

To incorporate disorder in this system, consider a cubic periodic array of lattice constant unity. In addition to experiencing force from the interparticle potential, each particle feels a random force f_i from the nearest lattice site. This is schematically shown in Fig. 1. In this figure, the disorder sites are marked in black, and are fixed at lattice sites of the imaginary mesh. The fluid particles are marked in red. The lattice sites push or pull A/B particles in opposite directions. The random field on each site is independent of time, and is chosen from a uniform distribution in the range $[-f, f]$. We have carried out simulations for various amplitudes (f) of the disorder.

The MD runs were performed using the standard velocity Verlet algorithm [30] with an integration time step $\Delta t = 0.01\tau$, where τ is the LJ time unit with $\tau = (m\sigma^2/\varepsilon)^{1/2} = 1$.

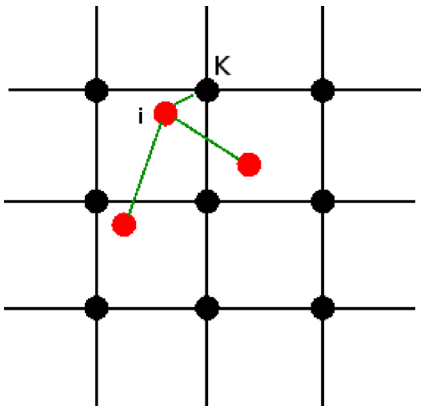

FIG. 1. (Color online) Schematic picture of the interactions in our system. The black circles indicate the disorder sites placed on a cubic lattice. The red (gray) circles indicate the fluid particles. A particle i interacts with the other fluid particles via the truncated LJ potential, and with the nearest disorder site (K, in this case) via a random field.

The temperature (T) was controlled by a Nosé-Hoover thermostat (NHT) [30], which is known to preserve hydrodynamics well. The force experienced by a particle includes a contribution from the discontinuous random field. This does not affect the integration of the equations of motion, as the NHT suppresses large fluctuations. Homogeneous initial configurations were prepared by equilibrating a system (without disorder) at $T = 10 \gg T_c$. At $t = 0$, the system is quenched to $T < T_c$, and is allowed to evolve towards the new equilibrium state.

For the characterization of the domain morphology, we obtain the correlation function

$$C(\vec{r},t) = \langle \psi(0,t)\psi(\vec{r},t)\rangle / \langle \psi(0,t)^2\rangle. \tag{3}$$

The order parameter $\psi(\vec{r},t)$ is defined on boxes of size $(2\sigma)^3$ as

$$\psi(\vec{r},t) = \frac{n_A(\vec{r},t) - n_B(\vec{r},t)}{n_A(\vec{r},t) + n_B(\vec{r},t)}, \tag{4}$$

where n_A and n_B are the local densities of A and B, respectively. The angular brackets in Eq. (3) represent statistical averaging. We also calculated the structure factor $S(\vec{k},t)$ ($\vec{k}$ being the wave vector), which is the Fourier transform of $C(\vec{r},t)$. As the system is isotropic, we consider the spherically averaged versions of $C(\vec{r},t)$ and $S(\vec{k},t)$, which are denoted as $C(r,t)$ and $S(k,t)$, respectively. Notice that we calculate the structure factor of the "density difference field" rather than the conventional structure factor of the "total density field." The average domain size, $\ell(t)$, was calculated from the first zero crossing of the correlation function. All statistical quantities were calculated from smoothed morphologies obtained by eliminating thermal fluctuations in *raw* configurations via a majority-rule procedure [31].

Our results for the disordered case were obtained from systems of $32\,768 (= 32^3)$ particles, after averaging over 40 independent runs at a quench temperature $T = 0.77T_c$. As stated earlier, this is far from the gas-liquid and solid-liquid transitions. Further, the temperature is sufficiently high that the system does not get trapped in metastable states. For each run, we used a distinct initial condition and disorder configuration. For reference, we also obtained results for pure systems (i.e., with $f = 0$) of $262\,144 (= 64^3)$ particles with averages over five independent runs, at the same quench temperature.

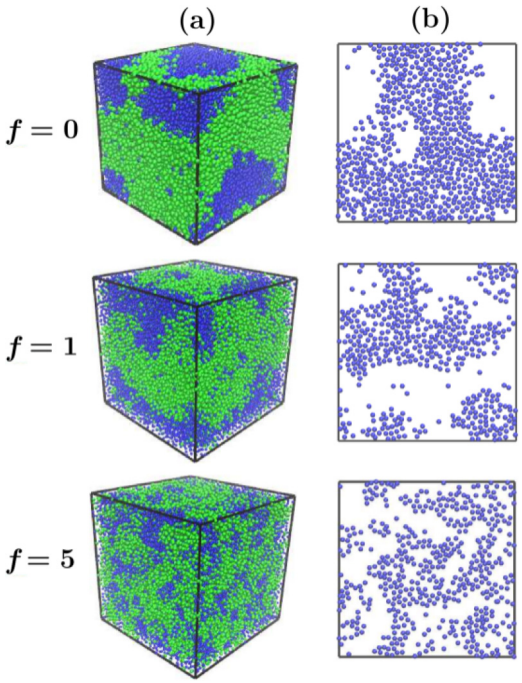

FIG. 2. (Color online) (a) Three-dimensional (size 32^3) snapshots of the fluid mixture at $t = 2000$ (LJ units), with different disorder amplitudes. The A and B particles are marked green (gray) and blue (black), respectively. (b) Two-dimensional (size 32^2) cross sections of the snapshots in (a). Here, only B particles are shown, for clarity.

In Fig. 2, we show the snapshots obtained at time $t = 2000$ during the phase separation of fluidic systems with $f = 0$ (pure case), 1, and 5. The $d = 3$ pictures, shown in Fig. 2(a), exhibit bicontinuous domain morphologies for all cases. However, it is evident that the growth gets appreciably slower with the increase of f. We will shortly quantify the slowing down of the domain growth law. Another noticeable feature in these pictures is that the domain boundaries roughen as the disorder amplitude increases. This can be better appreciated from Fig. 2(b), where we present the $d = 2$ cross sections of the snapshots in Fig. 2(a).

Next, let us quantify the properties of the morphologies depicted in Fig. 2. In Fig. 3(a), we present scaling plots of $C(r,t)$ vs r/ℓ from different times for the fluid system with $f = 2$. The neat collapse of data from different times demonstrates the self-similar nature of pattern formation during the kinetics of phase separation, even in the presence of disorder [3]. In Fig. 3(b), we present scaling plots of $C(r,t)$ vs r/ℓ at $t = 2000$ for different disorder amplitudes. Notice that the scaling function is strongly dependent on f, and becomes less oscillatory for larger f. Further, the $f = 0$ function decays linearly with r for small distances: $C(r,t) \simeq 1 - ar + \cdots$. This is the result of scattering from sharp interfaces, and is well known as the Porod law. On the other hand, the

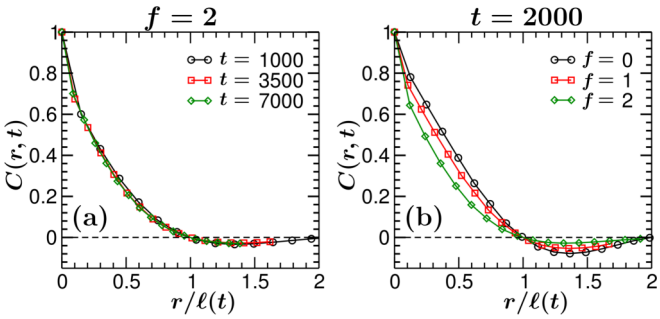

FIG. 3. (Color online) Scaling plots of the correlation function, $C(r,t)$ vs r/ℓ, for the fluid mixture. (a) Data sets for $f = 2$, at different times. (b) Data sets for $t = 2000$, at different disorder amplitudes. All times are measured in LJ units.

scaling functions for $f \neq 0$ display a distinct cusp behavior for $r \to 0$, which results from scattering off rough or fractal interfaces [32].

An important issue in disordered domain growth is that of *superuniversality* (SU), i.e., whether or not the dependence on disorder is only via the domain growth law. The SU property was demonstrated for the spatial correlation function and structure factor in early studies of nonconserved domain growth problems [12–15,17]. However, more recent studies [20,21] have shown the absence of SU in autocorrelation functions for these problems. The present communication clearly demonstrates that, for conserved growth problems with quenched random fields, SU does not apply even for the spatial correlation function.

In Fig. 4, we show the scaled structure factor plots corresponding to the correlation functions in Fig. 3(b). This figure confirms the breakdown of SU as the scaling functions depend strongly on disorder. The pure case obeys Porod's law: $S(k,t) \sim k^{-(d+1)}$ in momentum space [3]. On the other hand, the disordered cases show a marked non-Porod behavior, $S(k,t) \sim k^{-(d+\theta)}$ with $\theta \simeq 0.2$. This non-Porod behavior occurs due to scattering from rough interfaces with fractal

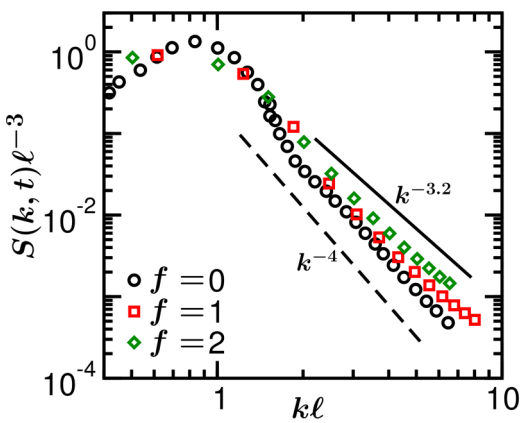

FIG. 4. (Color online) Scaling plots of the structure factor, $S(k,t)\ell^{-3}$ vs $k\ell$. The data sets correspond to three different values of f, as indicated, at $t = 2000$. The dashed line denotes the Porod law $[S(k,t) \sim k^{-(d+1)}]$ for scattering from sharp interfaces. The solid line corresponds to a non-Porod behavior $[S(k,t) \sim k^{-(d+\theta)}$ with $\theta = 0.2]$, which is characteristic of scattering from rough interfaces.

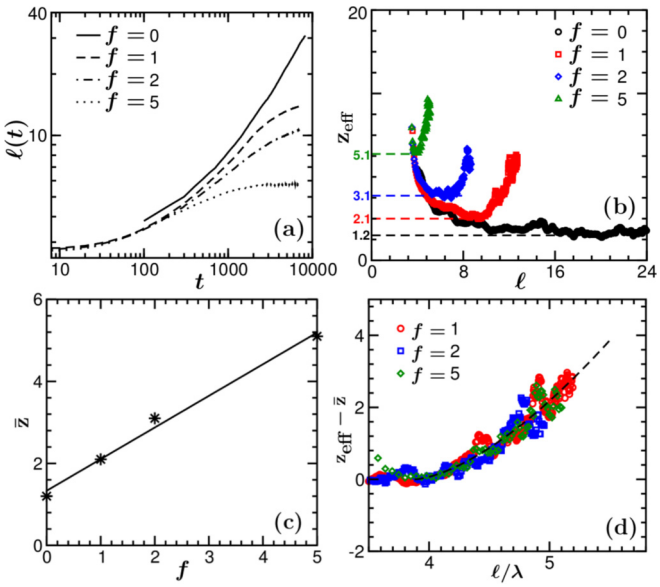

FIG. 5. (Color online) (a) Time dependence of domain size for different disorder amplitudes, plotted on a log-log scale. (b) Instantaneous dynamical exponent ($z_{\rm eff}$) vs ℓ for data sets in (a). The horizontal dashed lines mark the disorder-dependent intermediate-time exponent $\bar{z}$. (c) Plot of $\bar{z}$ vs f. The solid line denotes the best linear fit. (d) Plot of $z_{\rm eff} - \bar{z}$ vs ℓ/λ at late times ($z_{\rm eff} > \bar{z}$) for $f = 1,2,5$. The choice of λ is explained in the text. The dashed line denotes the best fit to Eq. (5).

dimension $d_f = d - \theta \simeq 2.8$ [33,34]. This is consistent with the value obtained in recent studies of ground-state morphologies in the $d = 3$ RFIM [32]. In general, we expect noninteger tails in the structure factor for domain growth problems with fractal interfaces resulting from quenched disorder.

Next, we analyze results for the time dependence of the domain size. In Fig. 5(a), we plot $\ell(t)$ vs t on a log-log scale for various disorder amplitudes. For the pure case ($f = 0$), our MD simulations are able to access the linear growth regime [8]. A slowing down in growth with increasing disorder amplitude is seen in Fig. 5(a)—this was already evident from the snapshots in Fig. 2. To quantify the growth, in Fig. 5(b) we plot the instantaneous dynamical exponent $z_{\rm eff} = 1/\alpha_{\rm eff}$ vs ℓ, where $\alpha_{\rm eff} = d(\ln \ell)/d(\ln t)$. For a power-law behavior, $\ell \sim t^{\alpha}$ and $z_{\rm eff} = 1/\alpha$. The result for the pure system saturates to the power law ($\alpha \simeq 1$) expected for the viscous hydrodynamic regime [8]. (The asymptotic inertial regime with $\alpha = 2/3$ has proven inaccessible to MD simulations as yet due to computational limitations.) However, for systems with disorder, $z_{\rm eff}$ does not show a similar behavior. In these cases, the growth obeys a power-law behavior at intermediate times (flat region of $z_{\rm eff}$ vs ℓ), while the long-time behavior is not power law. The exponent for this intermediate power-law behavior ($\bar{z}$) has an approximately linear dependence on the disorder amplitude (f), as shown in Fig. 5(c). In disordered systems, the interfaces tend to become locally trapped at energetically favorable sites. This gives rise to energy barriers, which are overcome by thermally activated hopping. The barrier dependence on ℓ determines the asymptotic domain growth law [9]. Our observation that $\bar{z}$ depends linearly on f is consistent with energy barriers

which have a logarithmic dependence on ℓ in this regime [17].

Finally, let us examine the asymptotic behavior of the length scale. Figure 5(b) shows a crossover to a regime where $z_{\rm eff}$ is ℓ dependent for the nonzero disorder cases. We use the method of Corberi *et al.* [21] to analyze the length scale in this regime. In Fig. 5(d), we plot $z_{\rm eff} - \bar{z}$ vs ℓ/λ, where λ is a disorder-dependent fitting parameter, which is chosen to obtain a neat data collapse. Our results (not shown here) are consistent with $\lambda \sim f^{-0.54}$, suggesting the scaling law $\lambda \sim f^{-1/2}$. However, this needs to be confirmed analytically. We look for a power-law behavior in the scaling function of Fig. 5(d):

$$z_{\rm eff} = \frac{d(\ln t)}{d(\ln \ell)} = \bar{z} + b\left(\frac{\ell - \ell_0}{\lambda}\right)^{\varphi}, \tag{5}$$

which fits well with the numerical data. The best-fit values for these parameters are $b \simeq 1.83 \pm 0.07$, $\ell_0 \simeq 3.88 \pm 0.02$, and $\varphi \simeq 1.54 \pm 0.03$. The corresponding growth law at long times is logarithmic with

$$\ell(t) \sim \lambda\left(\frac{\varphi}{b} \ln t\right)^{1/\varphi}. \tag{6}$$

The behavior of the growth law, i.e., a crossover from a disorder-dependent power law to a logarithmic behavior is consistent with previous studies for Ising systems with quenched disorder [20,21]. It is also in agreement with the analytical arguments of Ngamsaad *et al.* (NYT) [35], who studied phase-separation kinetics of fluids in a porous medium. Their model consisted of coupled partial differential equations for the order parameter field (advective Cahn-Hilliard equation) and the fluid velocity field (Brinkman-Darcy equation). NYT used a clever combination of physical arguments and dimensional analysis to obtain a logarithmic domain growth law due to hydrodynamic screening.

In summary, we have presented comprehensive MD results for the kinetics of phase separation in porous media, modeled by a LJ fluid in a random field. Here we studied domain growth in fluid mixtures with disorder and obtained three important results. First, the correlation functions and structure factors do not obey SU, i.e., the scaling functions explicitly depend on disorder. This is at variance with the corresponding result for nonconserved kinetics. Second, the structure factor shows a non-Porod tail in the disordered cases. This is characteristic of scattering from fractal interfaces with $d_f \simeq 2.8$. Third, the growth law shows a crossover from a preasymptotic regime with power-law growth ($\ell \sim t^{1/\bar{z}}$ where $\bar{z}$ increases linearly with disorder) to an asymptotic regime with logarithmic growth [$\ell \sim (\ln t)^{1/\varphi}$ with $\varphi \simeq 1.54$]. We do not see viscous hydrodynamic growth ($\ell \sim t$) in the disordered cases. However, an appropriate reduction of disorder amplitude (and a corresponding increase in system size) should recover viscous and inertial hydrodynamic regimes prior to the disordered logarithmic behavior. We hope that the results presented here will encourage further systematic experiments on this physically important system.

The authors acknowledge useful discussions with M. Zannetti, F. Corberi, and E. Lippiello. S.A. acknowledges UGC for financial support and JNCASR for hospitality during her visits. S.K.D. and S.A. acknowledge financial support from the Department of Science and Technology (DST), Government of India, via Grant No. SR/S2/RJN-13/2009. S.P. thanks DST for financial support via a J.C. Bose National Fellowship.

[1] K. Binder, in *Phase Transformation of Materials*, edited by R. W. Cahn, P. Haasen, and E. J. Kramer, Mater. Sci. Technol. (VCH, Weinheim, 1991), Vol. 5, p. 405.
[2] A. J. Bray, Adv. Phys. **43**, 357 (1994).
[3] *Kinetics of Phase Transitions*, edited by S. Puri and V. Wadhawan (CRC Press, Boca Raton, 2009).
[4] A. Onuki, *Phase Transition Dynamics* (Cambridge University Press, Cambridge, 2002).
[5] I. M. Lifshitz and V. V. Slyozov, J. Phys. Chem. Solids **19**, 35 (1961).
[6] E. D. Siggia, Phys. Rev. A **20**, 595 (1979).
[7] H. Furukawa, Phys. Rev. A **31**, 1103 (1985); **36**, 2288 (1987).
[8] S. Ahmad, S. K. Das, and S. Puri, Phys. Rev. E **82**, 040107(R) (2010); **85**, 031140 (2012).
[9] S. Puri, Phase Transitions **77**, 469 (2004).
[10] D. A. Huse and C. L. Henley, Phys. Rev. Lett. **54**, 2708 (1985).
[11] G. S. Grest and D. J. Srolovitz, Phys. Rev. B **32**, 3014 (1985); D. J. Srolovitz and G. S. Grest, *ibid.* **32**, 3021 (1985).
[12] S. Puri, D. Chowdhury, and N. Parekh, J. Phys. A **24**, L1087 (1991).
[13] S. Puri and N. Parekh, J. Phys. A **25**, 4127 (1992).
[14] S. Puri and N. Parekh, J. Phys. A **26**, 2777 (1993).
[15] A. J. Bray and K. Humayun, J. Phys. A **24**, L1185 (1991).
[16] M. Rao and A. Chakrabarti, Phys. Rev. Lett. **71**, 3501 (1993).
[17] R. Paul, S. Puri, and H. Rieger, Europhys. Lett. **68**, 881 (2004); Phys. Rev. E **71**, 061109 (2005).
[18] M. Henkel and M. Pleimling, Europhys. Lett. **76**, 561 (2006); Phys. Rev. B **78**, 224419 (2008).
[19] C. Aron, C. Chamon, L. F. Cugliandolo and M. Picco, J. Stat. Mech. (2008) P05016; L. F. Cugliandolo, Physica A **389**, 4360 (2010).
[20] E. Lippiello, A. Mukherjee, S. Puri, and M. Zannetti, Europhys. Lett. **90**, 46006 (2010); F. Corberi, E. Lippiello, A. Mukherjee, S. Puri, and M. Zannetti, J. Stat. Mech. (2011) P03016.
[21] F. Corberi, E. Lippiello, A. Mukherjee, S. Puri, and M. Zannetti, Phys. Rev. E **85**, 021141 (2012).
[22] F. Brochard and P. G. de Gennes, J. Phys. Lett. (Paris) **44**, 785 (1983).
[23] P. G. de Gennes, J. Phys. Chem. **88**, 6469 (1984).
[24] J. V. Maher, W. I. Goldburg, D. W. Pohl, and M. Lanz, Phys. Rev. Lett. **53**, 60 (1984).
[25] M. C. Goh, W. I. Goldburg, and C. M. Knobler, Phys. Rev. Lett. **58**, 1008 (1987).
[26] P. Wiltzius, S. B. Dierker, and B. S. Dennis, Phys. Rev. Lett. **62**, 804 (1989).

[27] S. K. Das, M. E. Fisher, J. V. Sengers, J. Horbach, and K. Binder, Phys. Rev. Lett. **97**, 025702 (2006).
[28] S. K. Das, J. Horbach, K. Binder, M. E. Fisher, and J. V. Sengers, J. Chem. Phys. **125**, 024506 (2006).
[29] S. Roy and S. K. Das, Europhys. Lett. **94**, 36001 (2011).
[30] D. Frenkel and B. Smit, *Understanding Molecular Simulations: From Algorithms to Applications* (Academic Press, San Diego, 2002).
[31] S. K. Das and S. Puri, Phys. Rev. E **65**, 026141 (2002).
[32] G. P. Shrivastav, S. Krishnamoorthy, V. Banerjee, and S. Puri, Europhys Lett. **96**, 36003 (2011); G. P. Shrivastav, M. Kumar, V. Banerjee, and S. Puri, Phys. Rev. E **90**, 032140 (2014).
[33] H. D. Bale and P. W. Schmidt, Phys. Rev. Lett. **53**, 596 (1984); A. J. Hurd, D. W. Schaefer, and J. E. Martin, Phys. Rev. A **35**, 2361 (1987).
[34] P.-Z. Wong, Phys. Rev. B **32**, 7417 (1985).
[35] W. Ngamsaad, J. Yojina, and W. Triampo, J. Phys. A **43**, 202001 (2010).